



Grain refining effect of Mg by novel particle cluster-containing Al–Ti–C master alloy

Xiao-teng LIU, Hai HAO, Xiao-xu ZHU, Xing-guo ZHANG

School of Materials Science and Engineering, Dalian University of Technology, Dalian 116024, China

Received 8 July 2014; accepted 25 March 2015

Abstract: A novel Al–Ti–C master alloy containing Al_4C_3 and TiC particle clusters, which exhibits great refining potential for Mg, was prepared. With the addition of 2% Al–Ti–C master alloy, the grains transform to equiaxed crystal with a diameter of (110 ± 17) μm . The results indicate that Al_4C_3 and TiC particle cluster, rather than a single particle, plays an important role in the refining process. Compared with the simplex smooth nucleating substrate, concave regions on the particle cluster provide easier route for the transformation from liquid Mg atoms to stable nucleus. Nucleus with a small size can also reach the critical nucleation radius when they attach on the concave regions of the substrate. Al_4C_3 and TiC particle clusters thus become more favorable nucleating substrate for α -Mg grains.

Key words: Mg; Al–Ti–C master alloy; particle cluster; grain refinement

1 Introduction

Mg alloys, as the excellent lightweight structure material, are receiving increasing attention in recent years [1–4]. In order to further broaden the application fields of Mg alloy, it is essential to improve their low strength and poor formability [5,6]. It is well-known that grain size is an important structural characteristic determining the mechanical properties. Many research works have been carried out to refine the grain size of Mg alloys, such as plastic deformation [7–9], imposing electromagnetic field [10] and applying modification treatment [11–13]. Some nucleating agents, C_2Cl_6 for instance, have been used in industry [11]. However, this method is often accompanied by harmful volatile matters released from the melt during the treatment [12]. It is therefore important to seek more effective and eco-friendly grain refining additives.

The current researches indicate that some inorganic carbon-containing agents, including carbon powders [11], Al_4C_3 [12], SiC [13] and carbon-bearing master alloys [14,15], exhibit positive refining effects. Among these agents, adding master alloy is one of the key options. Al–Ti–C master alloy, as an effective refiner for

Al alloy, has been investigated for many years. However, the study of its effect on Mg alloys is relatively less [16–18]. HAN et al [16] tried to introduce Ti element into Al–C melt to fabricate a series of Al–Ti–C master alloys with low Ti-to-C ratios by melt reaction method and investigated their refining performance on AZ31 alloy. The results indicate that Ti has a tendency to decrease the size and improve the distribution of Al_4C_3 particles. The refining effect mainly ascribes to heterogeneity nucleation on the Al-, C-, O-, Fe- and Mn-rich particles. KENNEDY et al [17] found that a lot of Al_4C_3 particles formed after the Al–TiC composite was treated at 700 °C for 48 h. Based on this, DING et al [18] prepared a new Al_4C_3 -containing grain refiner utilizing the destabilization of TiC and effectively refined AZ31 alloy. They suggest that Al_4C_3 particle could be a good substrate for α -Mg and B is essential in preparing Al_4C_3 -containing refiners by the TiC evolving method to avoid the poisoning effect of Ti.

From the literatures mentioned above, the phase composition and morphology in Al–Ti–C system rely heavily on the preparation method. In addition, most of the present studies focus on the “single-particle theory” for the nucleating of α -Mg and researches involving the refining potential of “particle cluster” are rarely

discussed. The purpose of the present work can be divided into two parts. The first part is to prepare Al–Ti–C master alloy containing Al_4C_3 and TiC particle clusters. The second part is to explore the potential of the obtained Al–Ti–C master alloys on refining α -Mg grains.

2 Experimental

The mixture of Mg powders (99% purity), Al powders (98% purity), Ti powders (99% purity) and graphite powders (99.85% purity) with a mass ratio of 2:3:2:1.5 was milled in a planetary ball mill for 12 h. Then 30 g of the mixture was cold-pressed into preforms with a diameter of 30 mm and dried in a furnace at 300 °C for 1 h. About 120 g of high purity Al (99.99% purity) was melt in a graphite crucible using the medium-frequency induction furnace at 1100 °C. Then the dried preform was added into the molten Al. The melt was stirred using a graphite rod for 30 s every interval of 10 min and poured into a preheated steel mold. The Al-based master alloy with the composition of 4.7% Ti, 3.5% C and 4.7% Mg, was finally obtained. Samples were sectioned from the final alloy and then prepared with standard metallographic procedure. The microstructures of the samples were examined by scanning electron microscope (SEM) after etching with Buswell's reagent. Phases were identified using XRD analysis.

A series of experiments were carried out to measure the refining effect of the fabricated Al–Ti–C master alloy. Pure Mg (99.95% purity) was adopted in the refining experiments to reduce the interference of other alloying elements. The Al–Ti–C master alloy with different amounts was added into the Mg melt at 760 °C. The melt was stirred for 60 s with a mild steel rod after holding for 25 min and then cast into a steel mold with a

diameter of 23 mm and a height of 45 mm. It should be noted that Al plays a positive role in refining Mg grains [19] and the Al–Ti–C master alloy contains a certain amount of Al. Thus, 1% pure Al (99.99% purity) was also used to refine Mg under the same condition to compare its efficiency with the master alloys. The samples produced thus were sectioned horizontally 10 mm from the bottom and then ground using SiC paper up to 4 μm . Standard polishing procedure was employed and then these samples were etched with a solution of picric and acetic acid (solution of 10 mL acetic acid, 10 mL H_2O , 4.2 g picric acid and 70 mL ethanol [20]) to reveal the grain boundaries. The micrographs presented in this work were all taken from the central region of the etched samples. The mean grain size was measured by linear intercept method. The schematic illustration of the experimental procedure is presented in Fig. 1.

3 Results

3.1 Phase composition and microstructures of Al–Ti–C master alloy

Figure 2 indicates that the Al–Ti–C master alloy mainly contains four phases, i.e., Al, Al_4C_3 , TiC and $\text{Mg}_{17}\text{Al}_{12}$. Al mainly ascribes to the Al matrix, and Al_4C_3 , TiC and $\text{Mg}_{17}\text{Al}_{12}$ phases derive from the reactions in the system. The phases can be further confirmed by SEM micrographs and EDS analysis, as shown in Fig. 3. Obviously, two kinds of particles disperse on the matrix. The black blocky phase is mainly composed of Al, C and O elements while the white cluster phase is mainly composed of Ti, C and Al elements. Considering that it is unlikely to form aluminum oxycarbides, such as Al_2CO and $\text{Al}_4\text{O}_4\text{C}$, the trace oxygen can be ascribed to the sample preparation [12,13]. The detected Al in the white cluster phase may come from the Al matrix beneath the

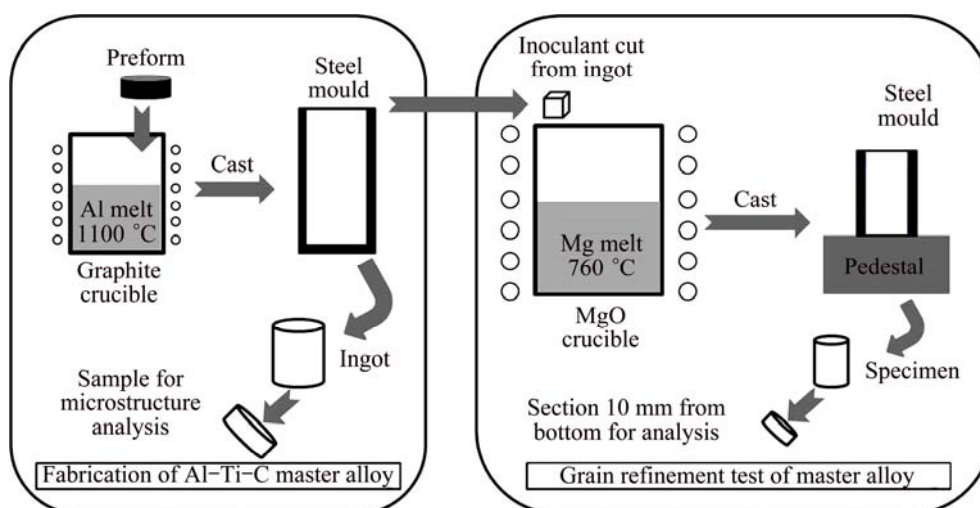


Fig. 1 Schematic illustration of experimental procedure

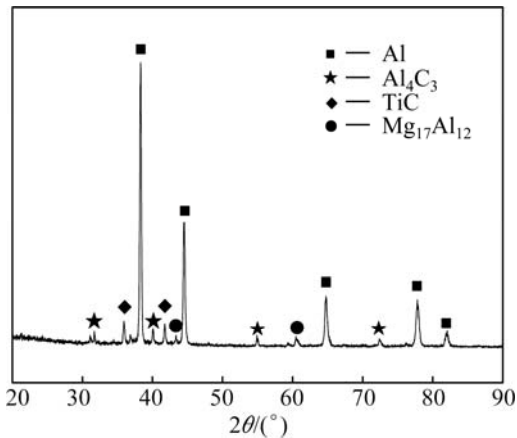


Fig. 2 XRD pattern of Al-Ti-C master alloy

particles due to the large volume of electron beam during the EDS testing. Combining the XRD analysis result, it can be confirmed that the black phase is Al_4C_3 and the white phase is TiC. It is worth noting that apart from a few isolated TiC particles, most of TiC particles attach to the surface of Al_4C_3 phase (Fig. 3(b)). This is so-called Al_4C_3 and TiC particle cluster.

3.2 Grain refining effect on Mg

Figure 4 exhibits the macro and micro photographs

of Mg with additions of 1% Al and 1%, 2%, 3% Al-Ti-C master alloy. Obviously, the Al-Ti-C master alloy shows much better performance than Al by comparing Figs. 4(a), (e) with (b), (f). With addition of 1% Al-Ti-C master alloy, the grain size further reduced by 67.5%, from (770 ± 346) μm to (250 ± 59) μm in contrast with that of 1% Al addition. No doubt, the extra Al introduced by the Al-Ti-C master alloy is not likely to play a dominant role. The particles in the master alloy have great effects. The black nuclei in the center of the grains (marked in circles in Figs. 4(f) and (g)) also preliminary prove this opinion. With the increase of the adding amount, the grains are further refined. The size of the grains declines to (110 ± 17) μm with addition of 2% Al-Ti-C master alloy. However, excess addition shows negative effects, as illustrated in Fig. 4(h). The average size is about (270 ± 67) μm .

SEM and EDS were employed to further analyze the particles in the center of the grains. Figure 5 exhibits a high resolution close-up of a α -Mg grain, whose center lies a particle cluster. The cluster shows the morphology of a black block surrounded by some white particles. EDS analysis results indicate that the black block mainly consists of Al, C, O elements while the white particles are mainly composed of Ti, C, Mg elements. Mg element may ascribe to the matrix. Considering the morphology

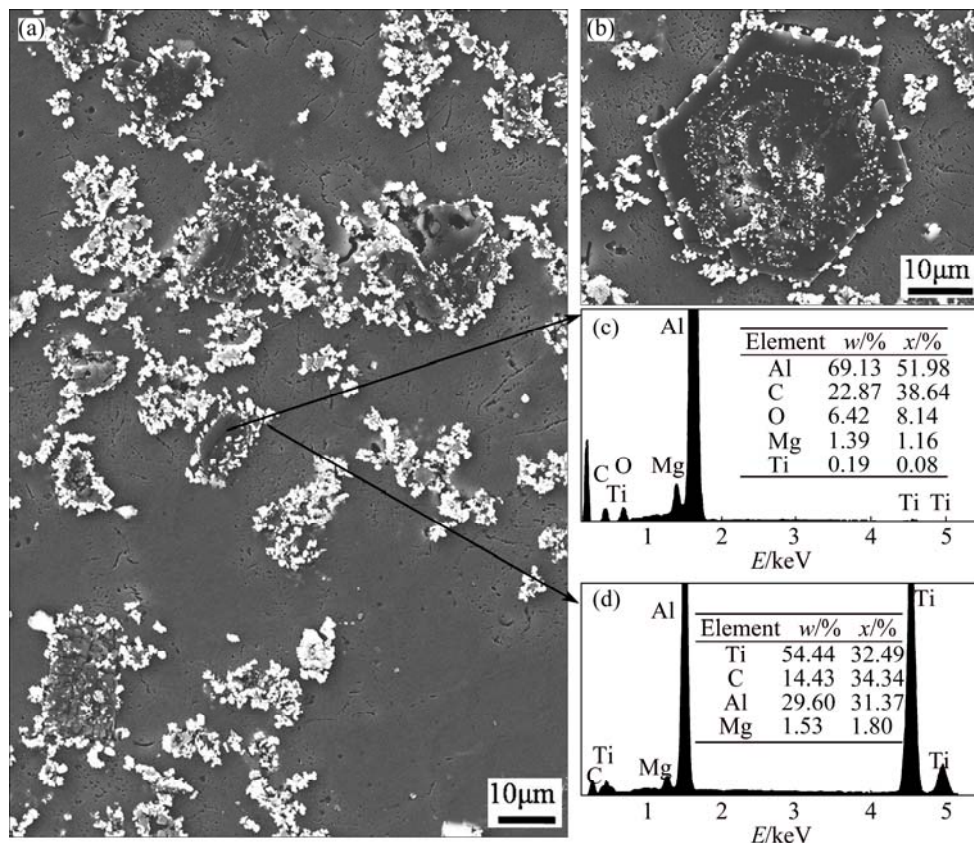


Fig. 3 SEM secondary electron images and EDS analysis results of Al-Ti-C master alloy: (a) Low magnification image of master alloy; (b) High magnification image of particle cluster; (c, d) EDS results

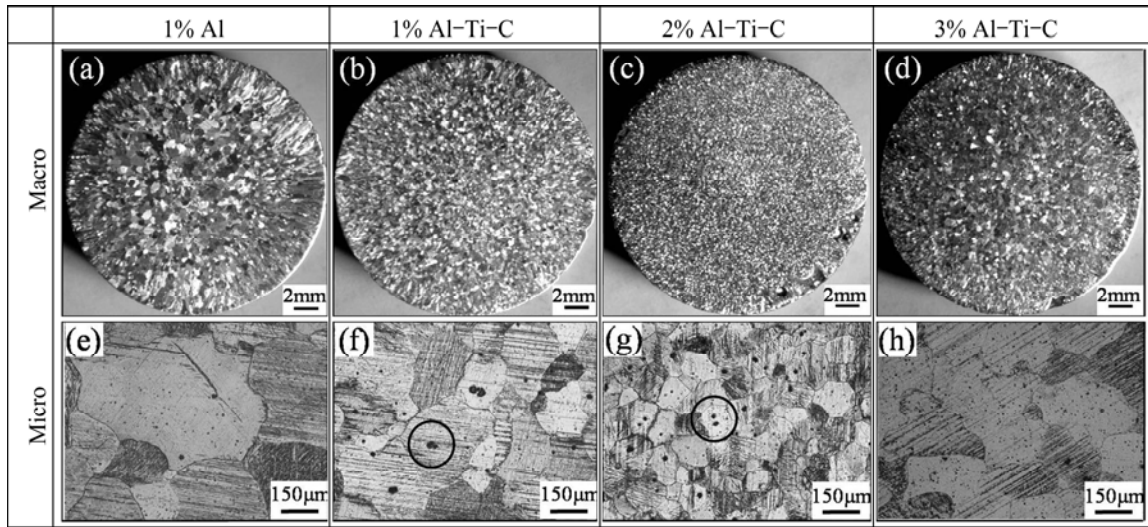


Fig. 4 Macro (a–d) and micro (e–h) photographs of Mg with additions of 1% Al and 1%, 2%, 3% Al–Ti–C master alloy

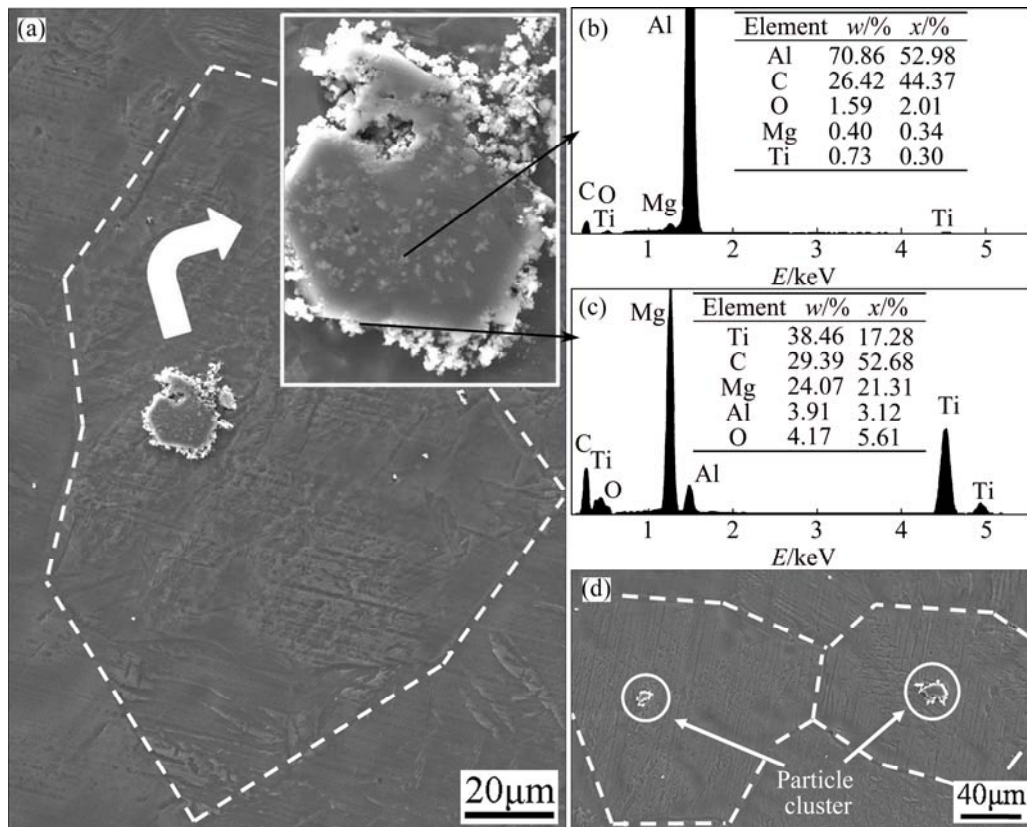


Fig. 5 SEM secondary electron images and EDS analysis results of particle cluster in Mg grain with 2% Al–Ti–C master alloy addition: (a) High magnification image of α -Mg grain; (b, c) EDS results; (d) Illustration of two grains with particle cluster

features, it can be deduced that the cluster consists of Al_4C_3 and TiC phases, which is introduced by the Al–Ti–C master alloy. It should be emphasized that the similar particle clusters were often observed in the α -Mg grains (Fig. 5(d)). Besides, some particle clusters located at the boundary of two (Fig. 6(a)) or three grains (Fig. 6(b)). The pervasive phenomenon indicates that the Al_4C_3 and TiC clusters do play important roles in refining α -Mg grains.

4 Discussion

4.1 Reaction mechanism of Al–Ti–C master alloy

The preparation of Al–Ti–C master alloy by the present method mainly contains two steps. Firstly, the exothermic reactions occur in the Al–Ti–C preform when the preheated preform is added into the Al melt. This is the critical step determining the final phase

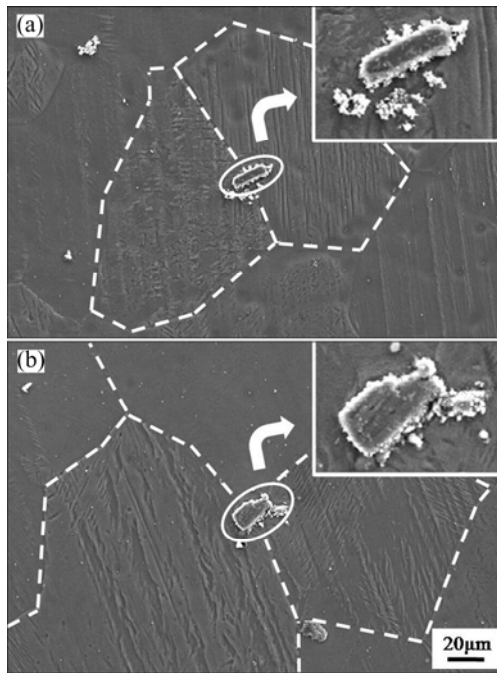
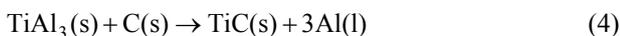
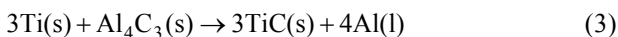


Fig. 6 SEM secondary electron images of particle clusters at boundary of grains: (a) Located at boundary of two grains; (b) Located at boundary of three grains

composition. Subsequently, the preform dissolves into the Al melt after the stirring process. The reaction mechanism in the Al–Ti–C system is really complex and the resultants rely heavily on the experiment condition and raw material components. According to the previous studies [16,21], the following four reactions may occur in the Al–Ti–C system in the present condition:



The temperature of the preform rises up after it is introduced into the Al melt. When the temperature reaches the melting point of Al, the Al powders in the preform melt and spread on the surface of solid Ti and graphite powders under the capillary force. The reaction between Al and Ti (Reaction 1) is activated at 780 °C [22]. This is the first reaction in the preform accompanied with massive heat release, which results in the sharp temperature increase of the preform. The bad wettability between Al and graphite will be obviously ameliorated in such condition [23] and the process of Reaction (2) to generate Al_4C_3 phase will be accelerated. Besides, the Al–C reaction to form Al_4C_3 is also exothermal [24], which will further contribute to the heat accumulation. Reaction (3) will be triggered at 890 °C [21]. With this reaction going on, TiC particles

form on the surface of Al_4C_3 phase and finally result in the formation of Al_4C_3 and TiC particle cluster. During the holding time, TiAl_3 phase transforms into TiC through Reaction (4). Thus, TiAl_3 has not been detected in the XRD analysis. After the stirring process, the particle phases in the preform dispersed in the Al melt and the Al–Ti–C master alloy was obtained. The Mg powders in the preform mainly act as the diluents in the Al–Ti–C system to promote the dilution of the particle phases during the stirring process [25]. In addition, Mg is in favor of meliorating the poor wettability between Al and graphite [26].

4.2 Grain refinement mechanism

It is commonly accepted that adding foreign nucleate substrate into the melt will decrease the nucleation energy and increase the nucleation probability, which finally leads to grain refinement [13]. Table 1 presents the lattice parameter and disregistry of Al_4C_3 , TiC with Mg. According to the classical nucleation theory, the nucleating substrate is believed to be ideal if the disregistry is less than 5% [27]. Both of Al_4C_3 and TiC fall in the very effective range for heterogeneous nucleation.

Table 1 Lattice parameter and disregistry of Al_4C_3 , TiC with Mg [12,23]

Particle	Crystallographic	Lattice parameter/nm	Disregistry in close-packed plane/%
Mg	HCP	$a=0.3208,$ $c=0.5209$	0
Al_4C_3	HCP	$a=0.3338,$ $c=2.4996$	4.05
TiC	Cubic	$a=0.4325$	4.7

However, the crystal structure is not the unique factor controlling the nucleating process. Some other factors, such as chemical factor and interfacial condition, are also important. For a certain nucleating substrate, the chemical factor (such as the interatomic bonding between different atoms) is difficult to be changed. Thus, the interfacial condition is even more important.

Based on the present study, when the temperature falls below the melting point, many nuclei will generate in the melt. Any nuclei with radius larger than the critical nucleation radius (r^*) will grow up and any with smaller radius will dissolve again [28]. Figure 7(a) represents the formation of α -Mg nuclei on two different substrates. The nuclei have the same contact angle (θ) with these two substrates, which indicates the same wettability between Mg melt and nucleating substrate. The parameter r^* is the critical nucleation radius under a certain cooling condition. Both of the nuclei reach the

critical nucleation radius and they will grow up steadily. However, the nucleus on concave substrate (Substrate 1) has smaller volume. This implies that nucleating substrate with concave surface enables smaller nucleus to reach the critical nucleation radius, which means a higher nucleating efficiency.

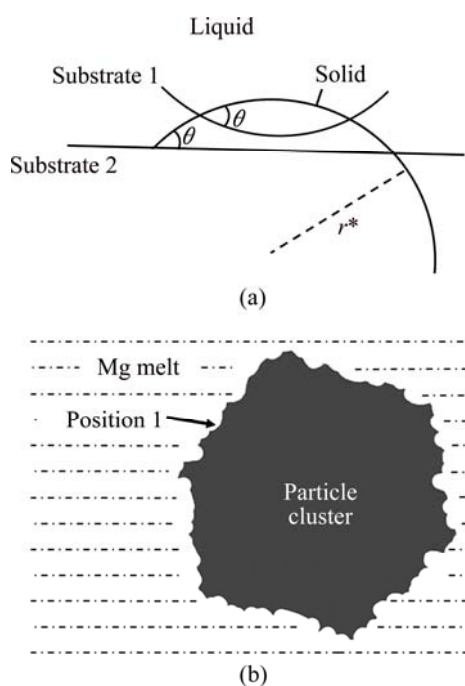


Fig. 7 Schematics of nuclei formation on different substrates (a) and particle clusters (b)

For the present study, the Al_4C_3 and TiC particle cluster is simplified as Fig. 7(b). The surface of the cluster is coarse, which contains many concave regions. Based on the analysis above, concave region (Position 1) is more favorable for the nucleation compared with a smooth surface. In addition, the rough surface increases the specific surface area of the substrate, which will improve the nucleating probability. Both of these enable Al_4C_3 and TiC particle cluster to be more potential nucleating substrate than simplex smooth substrate. Under the condition that only one nucleus forms on a particle cluster, the cluster locates at the center of the α -Mg grain (Fig. 5(d)). However, the particle cluster size is relatively large and the concave regions are sufficient. When two or more nuclei generate on a particle cluster simultaneously, the particle cluster will locate at the boundary of two or more α -Mg grains, as shown in Fig. 6.

There is a notable phenomenon that when the adding amount of the master alloy exceeds a proper level, the grains tend to be coarsening again. WANG et al [29] investigated the grain refinement limit of 6063 alloy inoculated by Al–Ti–C(B) master alloys and suggested that the massive release of solidification heat

occurring upon heterogeneous nucleation has vital influence on the nucleating process in the adjacent tiny area. Excessive nucleating site results in the interaction effect with each other, which will reduce the nucleating efficiency. In addition, the frequency of mutual collision, agglomeration and coalescence of the particle clusters may sharply increase. The coalescence will accelerate their sedimentation due to the density difference between the cluster and the melt and finally the effective substrate number decreases [30]. This is the reason why few nuclei were detected in the grains in Fig. 4(h).

It has to be pointed that pure Mg was adopted in this work to simplify the grain refining mechanism analysis by reducing the interference of other alloying elements. According to the experiment results and theoretical analysis, it is reasonable to deduce that the novel Al–Ti–C master alloy is also potential in refining Mg alloys and this will be verified in our following work.

5 Conclusions

- 1) A new Al–Ti–C master alloy, which contains Al_4C_3 and TiC particle clusters, was prepared. The master alloy shows enormous grain refining effect on Mg.
- 2) The particle clusters in the new Al–Ti–C master alloy are more favorable for the nucleating process. With TiC particles attaching on Al_4C_3 phase, a rough surface forms. The concave region on the substrate surface enables smaller nucleus to reach the critical nucleation radius and grow up steadily. In addition, the rough surface increases the specific surface area of the substrate and improves the nucleating probability. Both of these enable Al_4C_3 and TiC particle cluster to be potential nucleating substrate for α -Mg grains.

References

- [1] LI Ji-bao, WANG Feng, MAO Ping-li, LIU Zheng. Evolution of microstructure and tensile properties of extruded Mg–4Zn–1Y alloy [J]. *Journal of Rare Earth*, 2014, 32(12): 1189–1195.
- [2] WANG Ying-dong, WU Guo-hua, LIU Wen-cai, PANG Song, ZHANG Yang, DING Wen-jiang. Influence of heat treatment on microstructures and mechanical properties of gravity cast Mg–4.2Zn–1.5RE–0.7Zr magnesium alloy [J]. *Transactions of Nonferrous Metals Society of China*, 2013, 23(12): 3611–3620.
- [3] DU Jun, WANG Ming-hua, ZHOU Ming-chuan, LI Wen-fang. Evolutions of grain size and nucleating particles in carbon-inoculated Mg–3% Al alloy [J]. *Journal of Alloys and Compounds*, 2014, 592: 313–318.
- [4] XU Tian-cai, PENG Xiao-dong, JIANG Jun-wei, XIE Wei-dong, CHEN Yuan-fang, WEI Guo-bing. Effect of Sr content on microstructure and mechanical properties of Mg–Li–Al–Mn alloy [J]. *Transactions of Nonferrous Metals Society of China*, 2014, 24(9): 2752–2760.
- [5] ZHANG Yu, WU Yu-juan, PENG Li-ming, FU Peng-huai, HUANG Fei, DING Wen-jiang. Microstructure evolution and mechanical

- properties of an ultra-high strength casting Mg–15.6Gd–1.8Ag–0.4Zr alloy [J]. *Journal of Alloys and Compounds*, 2014, 615: 703–711.
- [6] ZHANG Li, ZHANG Jing-huai, XU Chi, LIU Shu-juan, JIAO Yu-feng, XU Long-jiang, WANG Yan-bo, MENG Jian, WU Rui-zhi, ZHANG Mi-lin. Investigation of high-strength and superplastic Mg–Y–Gd–Zn alloy [J]. *Materials and Design*, 2014, 61: 168–176.
- [7] GONG Xi-bing, LI Hao, KANG S B, CHO J H, LI Sai-yi. Microstructure and mechanical properties of twin-roll cast Mg–4.5Al–1.0Zn alloy sheets processed by differential speed rolling [J]. *Materials and Design*, 2010, 31(3): 1581–1587.
- [8] GONG Xi-bing, KANG S B, LI Sai-yi, CHO J H. Enhanced plasticity of twin-roll cast ZK60 Mg alloy through differential speed rolling [J]. *Materials and Design*, 2009, 30(9): 3345–3350.
- [9] LIU Xuan, HU Wen-yi, LE Qi-chi, ZHANG Zhi-qiang, BAO Lei, CUI Jian-zhong. Microstructures and mechanical properties of high performance Mg–6Gd–3Y–2Nd–0.4Zr alloy by indirect extrusion and aging treatment [J]. *Materials Science and Engineering A*, 2014, 612: 380–386.
- [10] WANG Bin, YANG Yuan-sheng, SUN Ming-li. Microstructure refinement of AZ31 alloy solidified with pulsed magnetic field [J]. *Transactions of Nonferrous Metals Society of China*, 2010, 20(9): 1685–1690.
- [11] YANO E, TAMURA Y, MOTEGI T, SATO E Y, MOTEGI T, SATO E. Effect of carbon powder on grain refinement of an AZ91E Mg alloy [J]. *Materials Transactions*, 2003, 44(1): 107–110.
- [12] LU L, DAHLE A K, STJOHN D H. Grain refinement efficiency and mechanism of aluminium carbide in Mg–Al alloys [J]. *Scripta Materialia*, 2005, 53(5): 517–522.
- [13] LU L, DAHLE A K, STJOHN D H. Heterogeneous nucleation of Mg–Al alloys [J]. *Scripta Materialia*, 2006, 54(12): 2197–2201.
- [14] LIU Sheng-fa, ZHANG Yuan, HAN Hui. Role of manganese on the grain refining efficiency of AZ91D magnesium alloy refined by Al_4C_3 [J]. *Journal of Alloys and Compounds*, 2010, 491: 325–329.
- [15] MA Guo-long, HAN Guang, LIU Xiang-fa. Grain refining efficiency of a new Al–1B–0.6C master alloy on AZ63 magnesium alloy [J]. *Journal of Alloys and Compounds*, 2010, 491: 165–169.
- [16] HAN Guang, LIU Xiang-fa, DING Hai-min. Grain refinement of AZ31 Mg alloy by new Al–Ti–C master alloys [J]. *Transactions of Nonferrous Metals Society of China*, 2009, 19(5): 1057–1064.
- [17] KENNEDY A R, WESTON D P, JONES M I. Reaction in Al–TiC metal matrix composites [J]. *Materials Science and Engineering A*, 2001, 316(1): 32–38.
- [18] DING Hai-min, LI Hui, LIU Xiang-fa. Different elements-induced destabilisation of TiC and its application on the grain refinement of Mg–Al alloys [J]. *Journal of Alloys and Compounds*, 2009, 485: 285–289.
- [19] LEE Y C, DAHLE A K, STJOHN D H. The role of solute in grain refinement of Mg [J]. *Metallurgical and Materials Transactions A*, 2000, 31(11): 2895–2906.
- [20] ZHANG Ai-min, HAO Hai, ZHANG Xing-guo. Grain refinement mechanism of Al–5C master alloy in AZ31 magnesium alloy [J]. *Transactions of Nonferrous Metals Society of China*, 2013, 23(11): 3167–3172.
- [21] KENNEDY A R, WESTON D P, JONES M I, ENEL C. Reaction in Al–Ti–C powders and its relation to the formation and stability of TiC in Al at high temperatures [J]. *Scripta Materialia*, 2000, 42(12): 1187–1192.
- [22] HOU Yun-feng. Structure micro kinetics of combustion synthesis Al–Ti–C and grain refining performance evaluation [D]. Lanzhou: Lanzhou University of Technology, 2007: 42–52. (in Chinese)
- [23] XU Chun-xiang. Research on synthesis and grain refining efficiency of Al–Ti–C based master alloy [D]. Taiyuan: Tiyuan University of Technology, 2010: 38–39. (in Chinese)
- [24] WANG Zhen-qing, LIU Xiang-fa, ZHANG Jun-yan, BIAN Xiu-fang. Study of the reaction mechanism in the Al–C binary system through DSC and XRD [J]. *Journal of Materials Science*, 2004, 39: 2179–2181.
- [25] WANG Hui-yuan, ZHAO Feng, JIANG Qi-chuan, WANG Yan, MA Bao-xia. Effect of Mg addition on the self-propagating high temperature synthesis reaction in Al–Ti–C system [J]. *Journal of Materials Science*, 2005, 40: 1255–1257.
- [26] EUSTATHOPOULOS N, JOUD J C, DESRE P. The wetting of carbon by aluminum and aluminum alloys [J]. *Journal of Materials Science*, 1974, 9: 1233–1242.
- [27] MURTY B S, KORI S A, CHAKRABORTY M. Grain refinement of aluminium and its alloys by heterogeneous nucleation and alloying [J]. *International Materials Reviews*, 2002, 47(1): 3–29.
- [28] TURNBULL D. Formation of crystal nuclei in liquid metals [J]. *Journal of Applied Physics*, 1950, 21: 1022–1028.
- [29] WANG En-zhao, GAO Tong, NIE Jin-feng, LIU Xiang-fa. Grain refinement limit and mechanical properties of 6063 alloy inoculated by Al–Ti–C(B) master alloys [J]. *Journal of Alloys and Compounds*, 2014, 594: 7–11.
- [30] CHEN Ting-jun, WANG Rui-quan, HUANG Hai-jun, MA Ying, HAO Yuan. Grain refining technique of AM60B Mg alloy by $MgCO_3$ [J]. *Transactions of Nonferrous Metals Society of China*, 2012, 22(7): 1533–1539.

含有颗粒团的 Al–Ti–C 中间合金对镁的细化作用

刘晓滕, 郝海, 朱小旭, 张兴国

大连理工大学 材料科学与工程学院, 大连 116024

摘要: 制备一种含有 Al_4C_3 和 TiC 颗粒团的 Al–Ti–C 中间合金, 该合金对纯镁有很好的细化作用。当中间合金加入量为 2% 时, 镁晶粒细化为 $(110 \pm 17) \mu\text{m}$ 的等轴晶。通过分析可知, Al_4C_3 和 TiC 组成的颗粒团在细化过程中发挥了重要作用。与单个、光滑的形核颗粒相比, 颗粒团上的凹面区域增加了熔体中的液态镁原子向稳定晶核转变的可能性, 依附在颗粒团凹面区域尺寸较小的晶胚也可以满足临界形核半径的要求, 这使得 Al_4C_3 和 TiC 颗粒团成为镁晶粒更理想的形核基底。

关键词: 镁; Al–Ti–C 中间合金; 颗粒团; 晶粒细化

(Edited by Xiang-qun LI)